

Synergetic Model of Electro-friction Interaction

Igor Plokhov

Department of Electric Drive and Automation Systems
Pskov State University
Pskov, Russia
igor_plokhov@list.ru

Igor Savraev

Department of Electric Drive and Automation Systems
Pskov State University
Pskov, Russia
igor_savraev@mail.ru

Alexander Ilyin

Department of Electric Drive and Automation Systems
Pskov State University
Pskov, Russia
al.ilyin@yandex.ru

Nikita Kotkov

Department of Electric Drive and Automation Systems
Pskov State University
Pskov, Russia
4ce@goodgame.ru

Oksana Kozyreva

Department of Electric Drive and Automation Systems
Pskov State University
Pskov, Russia
ks_33n@mail.ru

Abstract—The paper describes algorithms and structure of the electro-friction interaction synergetic model. The results of theoretical modelling and experimental study of sliding electrical contact are given. The comparison of theoretical and experimental results made in the paper proves high validity of the model and its programmatic implementation.

Keywords—fractal theory, simulation modelling, sliding contact, synergetic.

I. INTRODUCTION

The basic approaches to the modern explanation of the physical processes in the sliding electrical contact are the next.

A common surface of two contacting rough bodies divides into many separate spots. When the flow of energy gets through the surface, it overcomes additional constriction resistance because of the nonuniform flow lines. In addition, there is the resistance of the surface films.

The theory of the electro-frictional interaction (EFI) at the time is at a critical time when there are large bulk of experimental data, hypotheses and different models, which could not be adequate to the studied processes. To overcome this conflict the new physical views and presentations must be involved in the applied area.

At present it is developing synergetics, the theory of self-organizing systems, and fractal theory studying self-similar evolutionary structures that cannot be described within Euclidian geometry.

Synergetics is studying the processes of the self-organizing, stability and disintegration of different nature structures forming in the open systems and the ordered state of which is connected to cooperative behaviour of their subsystems. This leads to the forming of self-organizing structures as the result of energy and material exchange with the environment when equilibrium has established of the entropy production and reduction [1] –

[5]. The evolution of a system is considered as transition through the series of thermodynamic quasi-equilibrium states [6]. Fractal theory [7] – [10] has become the base for quantitative description of the self-organizing structures using the fractal dimension as a parameter.

II. MODEL OF SLIDING CONTACT TRANSIENT LAYER

The transient layer of sliding electric contact (SC) is representable as set of the contact elements (CE) placed in nodes of a regular grid on the transitional plane (TP). We will describe each CE with the state vector having components.

Components of the power vector F are independent input influences: pressure force F_p , velocity of relative movement in contact couple of v , external voltage applied to contact U , environment temperature θ_{env} , vector of concentration of environment chemical reagents Z .

We will divide all components of the state vector of a contact element into the following classes. Mechanical V_M : contact stiffness S_C ; contact damping K_C ; contact approach Y_C ; contact force F_C ; microhardness q ; density ρ ; coefficient of boundary friction k_{fr} . Electrical V_E : voltage U (it is identical for all contact elements); fritting voltage U_f ; electric conductance g_E or resistance ρ_E ; contact capacity C_E ; current I through C_E . Thermal V_T : heat capacity C_θ ; heat conductivity k ; melting temperature θ_m ; evaporation temperature θ_{ev} ; CE temperature θ . Chemical V_H : vector of chemical composition h ; intensity of the main chemical reactions of V_h .

Let's determine the state vector by the sum of this four components

$$V = V_M + V_E + V_\theta + V_H \quad (1)$$

Voltage U is identical for all CE, however the value of current will be different for the different types and characteristics of conductivity, different temperatures, approaches, and etc. Besides, the flow of current leads to emitting power in CE and increases temperature θ ,

Print ISSN 1691-5402
Online ISSN 2256-070X

<http://dx.doi.org/10.17770/etr2019vol3.4072>

© 2019 Igor Plokhov, Alexander Ilyin, Oksana Kozyreva, Igor Savraev, Nikita Kotkov.
Published by Rezekne Academy of Technologies.

This is an open access article under the Creative Commons Attribution 4.0 International License.

which significantly affects conductivity of the element and conductivity of the neighbor areas.

In each CE there are substances and compounds of different concentration which can react with each other and with the materials of contact bodies. Either they can be passive or be catalysts and inhibitors for other reactions.

III. MODIFICATION OF THE STATE VECTOR COMPONENTS

The operations described below provide a basis for the dynamic processes in CE and contain the main computational procedures.

In the transient layer matrix we allocate clusters of direct and film conductivity (α -clusters and β -clusters). For this we use an allocation procedure that translates the elements of each cluster into an additional matrix.

After calculating the number of elements that make up the cluster N_i we calculate the characteristic radius of the cluster r_{cl} as the gyration radius R_g :

$$R_g = \sqrt{\frac{1}{N} \sum_{i=1}^N r_i^2} = \sqrt{\frac{1}{N} \sum_{i=1}^N [(X_c - x_i)^2 + (Y_c + y_i)^2]} \quad (2)$$

$$X_c = \sqrt{\frac{1}{N} \sum_{i=1}^N x_i}, Y_c = \sqrt{\frac{1}{N} \sum_{i=1}^N y_i} \quad (3)$$

Determine the fractal dimension of the cluster by the formula

$$D = \frac{\lg N}{\lg r_{cl} - \lg r} \quad (4)$$

Find the resistance of each cluster as the sum of the constriction resistances of the sliding contact upper and lower half-spaces, the resistance of the oxide film and the wear products $R_{cli} = R_{ci}' + R_{ci}'' + R_{fi} + R_{wp}$, where:

$$R_{ci}' = \frac{\rho E'}{4Dr_{ci}}, R_{ci}'' = \frac{\rho E''}{4Dr_{ci}}. \quad (5)$$

Calculate the contact resistance as a parallel connection of all clusters:

$$R = (\sum R_{cli}^{-1})^{-1} \quad (6)$$

Calculate the full contact current (R_{br} is the resistance of the brush body)

$$I = \frac{U}{R_{br} + R} \quad (7)$$

Find the thermal power emitting in each cluster. Power contains electrical and mechanical components.

Electrical component:

$$P_{Ei} = \frac{\Delta U^2}{2R_{cli}} \quad (8)$$

$$\Delta U = U - IR_{br} \quad (9)$$

where ΔU is the voltage drop at the transient layer; U is the voltage applied to the contact pair; I is the current of SC; R_{br} is the brush resistance.

Mechanical power of friction:

$$P_{Mi} = S_{Ci} + \Delta Y_i k_{fr} v, \quad (10)$$

where S_C is the CE stiffness, N/m; ΔY is the compression of CE, m; k_{fr} is the friction coefficient; v is the velocity of microreliefs displacement, m/s.

Then the total power in CE is

$$P_{CEi} = P_{Ei} + P_{Mi}. \quad (11)$$

Determine the CE temperature increment for one step of modelling time. Since the emitting power is went into heating the CE volume to a temperature θ over a time Δt , then using the electrothermal analogy method [11] – [15] an equivalent electrical circuit can be made. The heat source of power P_{CE} will be represented as the current source I_E and the heat capacity of CE C_{CE} as the electrical capacitance C_E and the voltage U_E corresponds to the temperature θ (Fig. 1). Write in the operator form:

$$U_E(p) = I_E X_C(p) = \frac{I_E}{pC_E} \quad (12)$$

where $X_C = \frac{1}{pC_E}$ is the reactance of the capacitor C_E .

In accordance with the direct analogy:

$$\theta(p) = \frac{P_{CE}}{pC_{CE}}, C_{CE} = C_{CE} m_{CE} c_{CE}, \quad (13)$$

where c_{CE} is the specific heat; $m_{CE} = \Delta x^2 \Delta h \rho_{CE}$ is the mass of CE; Δh is the CE height; ρ_{CE} is the average density of the CE materials

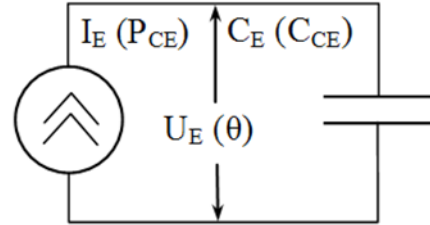


Fig. 1. Equivalent circuit.

$$\text{After } \theta(t) = \frac{P_{CE}}{C_{CE} \Delta x^2 \Delta h \rho_{CE}} t; \text{ get:} \quad (14)$$

$$\text{Repre: } \Delta \theta = \frac{P_{CE}}{C_{CE} \Delta x^2 \Delta h \rho_{CE}} \Delta t; \text{ rences:} \quad (15)$$

By the one step of the simulation the CE temperature will be:

$$\theta_{i+1} = \theta_i + \Delta \theta \quad (16)$$

The temperature of the CE has been changed due to heat exchange with the contacting bodies and the neighbour CE. Therefore, after calculating the temperature increment caused by heat emitting in CE, we calculate the temperature distribution in the three-dimensional system of nodes over the same time interval (Fig. 2) using the explicit method [12], [13].

Taking into account the nonuniform distribution of thermal conductivity and heat capacity in the structure of the transition layer, we can write:

$$\theta_{i,j,s}(t + \Delta t) = \left\{ \begin{array}{l} \theta_{i,j,s}(t) + \\ F_{i+1,j,s}(t)\Delta\theta_{i+1,j,s}(t) + \\ F_{i-1,j,s}(t)\Delta\theta_{i-1,j,s}(t) + \\ F_{i,j+1,s}(t)\Delta\theta_{i,j+1,s}(t) + \\ F_{i,j,s+1}(t)\Delta\theta_{i,j,s+1}(t) + \\ F_{i,j,s-1}(t)\Delta\theta_{i,j,s-1}(t) \end{array} \right\}, \quad (17)$$

where $\theta_{i,j,s}(t)$ is the temperature of the node with coordinates i, j, s ; $\Delta\theta_{i+1,j,s}(t) = \theta_{i+1,j,s}(t) - \theta_{i,j,s}(t)$, $\Delta\theta_{i-1,j,s}(t) = \theta_{i-1,j,s}(t) - \theta_{i,j,s}(t)$, and etc. are the temperature differences of the calculated node

and the neighbor nodes; $F_{i,j,s} = \frac{\langle k_{i,j,s} \rangle}{\langle c_{i,j,s} \rangle \Delta x^2 \langle \rho_{i,j,s} \rangle} \Delta t$ is Fourier number for the calculated node, where $\langle k_{i,j,s} \rangle$, $\langle c_{i,j,s} \rangle$, $\langle \rho_{i,j,s} \rangle$, are the average values of thermal conductivity, specific heat and density calculated by the nodes of the fragment (Fig. 2).

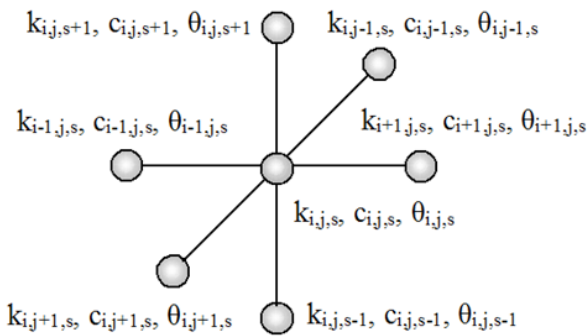


Fig. 2. Calculation of the sliding contact non-stationary temperature field.

The computational procedure has a stable solution if the Fourier number is less or equal 1/6 [12]. This indicator has the greatest value for the zones of direct conduction, therefore the choice of the step Δt and the discretization Δx are made by CE allocated into the specified zones.

The temperature increment of the CE from electromechanical heat emitting and its change due to the distribution of heat over the three-dimensional grid is not combined into a general procedure, since in this case the principle of simultaneous heat emitting in CE is violated. The calculation of the non-stationary temperature field of the SC is carried out for each Δt in two steps and for analysis we use only the final values of the CE temperatures for the second step.

To simplify the algorithm and increase the speed, we introduce the assumption that the temperature of the CE layers adjacent to the contact is defined as the half sum of the average temperature of all calculated CE of the transient layer and the temperatures of the contacting bodies. We also neglect the convective heat transfer at the

boundaries of the contact layer setting zero values of the thermal conductivity of boundary CE to the environment.

At each step of calculating the temperature field for all CE, we check the condition for exceeding the critical temperature levels of materials: 1) the recrystallization temperature, 2) melting point, 3) the evaporation temperature. Depending on which interval the temperature of the calculated CE falls within, it is decided how to change its characteristics and parameters.

Up to the temperature θ_m the mechanical stiffness of the CE is considered constant. In the interval $\theta \in [\theta_m, \theta_{ev}]$, the stiffness of the CE is changing in linear dependence. When the temperature θ_{ev} is reached evaporation of the least heat-resistant material of the CE occurs and the distance between the contacting surfaces at this point increases. For this a correction is made in the matrix of micro-reliefs. The approach in CE is changed by the value of Δh . As a result at a constant pressing force F_n the equivalent stiffness of the SC $C_{k\alpha}$ changes and the approach of the contacting surfaces is:

$$\Delta Y = \frac{F_b}{S_{CE}}, \quad (18)$$

where $S_{CE} = \sum S_{C_i}$.

As the temperature increases the conductivity of the surface films also increases and when the certain temperature $\theta = \theta_{tb}$ is reached thermal breakdown occurs, which is defined as the transition of the CE to the direct conductivity state.

The fritting of oxide films is interpreted as the transition of the CE into the direct conduction state when the electric field strength reaches the threshold value E_f that depends on the voltage at the contact layer and the thickness of the oxide film: $E = \frac{\Delta U}{d}$.

If $E > E_f$ CE goes into the direct conduction state.

The temperature dependence of the specific resistance, specific heat capacity, thermal conductivity and friction power is taken into account using

$$\rho_E = \rho_{E0} (1 + \alpha \Delta T), \quad (20)$$

$$c = c_0 (1 + \alpha_c \Delta T), \quad (21)$$

$$P_M(T) = P_{M0} \left(1 - \left(\frac{\Delta T}{T^* - T_0} \right)^2 \right), \quad (22)$$

where ρ_{E0} is the electrical resistivity at the initial temperature; α is the temperature coefficient of resistance, $1/K$; ΔT is the difference between the current and initial temperatures; c_0 and k_0 are specific heat and thermal conductivity at the initial temperature; α_c and α_k are the temperature coefficients of specific heat and thermal conductivity; coefficient α_k may be, both positive and negative, depending on the materials of the SC; P_{M0} is the

friction power at the initial temperature; T is the current temperature; n and T_* are the parameters which selected from the condition of the best approximation of the empirical dependence $P_M(T)$ in the studying temperature range.

The block diagram Fig. 3 depicts the main procedures of the simulation program. The main loop contains the block “Service input-output operations”, which is responsible for the graphical interfaces of the program, the visualization of tables, graphs and color portraits, etc.

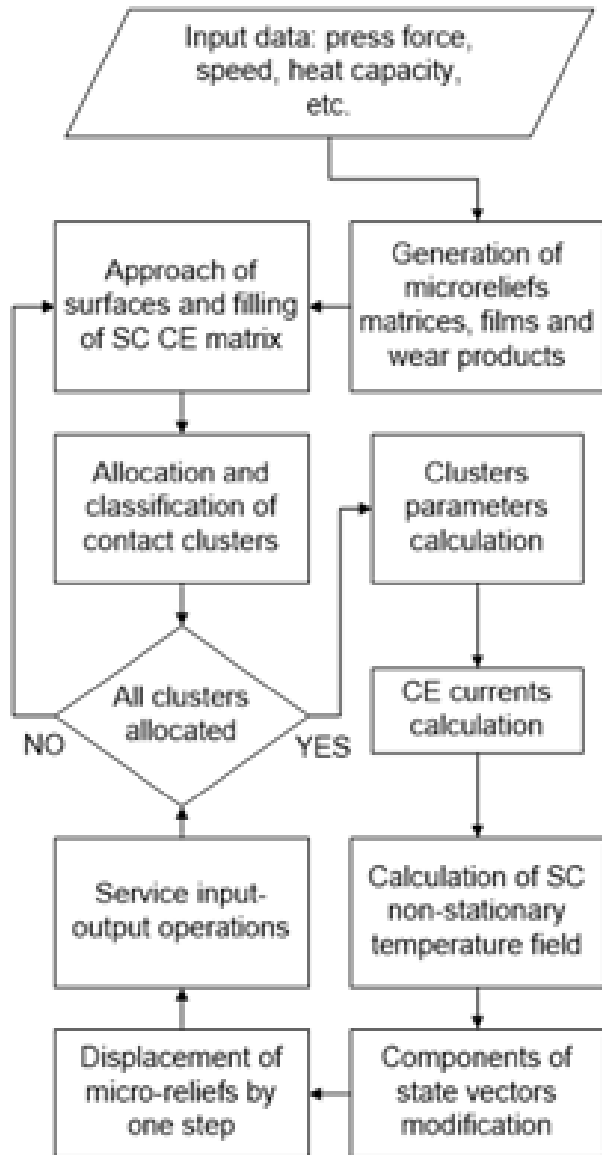


Fig. 3. Generalized block diagram of the EFI simulation model.

IV. THEORETICAL AND EXPERIMENTAL STUDY OF EFI DYNAMIC PROCESSES

Objectives of the study are: 1) determination of the simulation model adequacy, 2) study of the qualitative regularities of the EFI dynamics related to the processes of formation and growth of conducting clusters in the transition layer, thermal processes and voltage-current dependencies generated by various disturbing influences. Similar studies are described in [16] – [22].

Let's compare some model and experimental

characteristics.

The calculated voltage-current attractor shown in Fig. 4 is obtained with a sinusoidal modulation of the pressing force in the range from 2 to 25 N at the applied voltage 2 V and the speed of 3000 rpm for the contact pair “brush-steel ring”. Under the same conditions the experimental voltage-current limit cycle is shown in Fig. 5. The main difference is that the modulation of the pressing force in the experiment occurred naturally as the result of the interaction of the brush with the irregularities of the contact surface. In addition there was an effect of screw thread of the steel ring on the contact area value. The randomness of the phase trajectory shown in Fig. 5 is explained by the result of the action of these two polyharmonic factors. Despite all its complexity the indicated trajectory was steadily reproduced on each revolution of the ring with the slight stochastic variations.

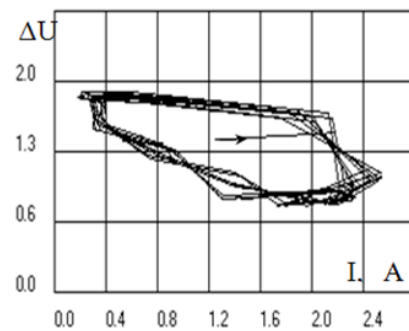


Fig. 4. Calculated voltage-current attractor.

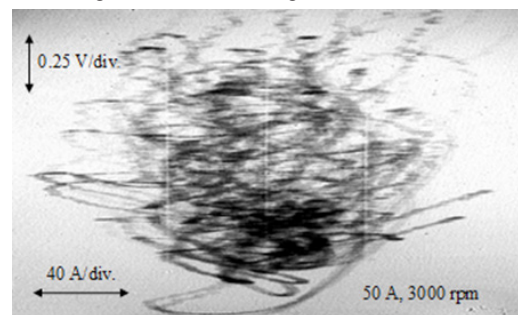


Fig. 5. Experimental voltage-current attractor.

Statistical estimates of these curves is the ranges of current I and voltage drop ΔU are almost match. For I_{exp} the range of variation is about 200 A and for I_{calc} the range is calculated as $2.3 \cdot 89 = 204.3$ V. For ΔU_{exp} and ΔU_{calc} the ranges are quite close.

In the Fig. 6 the model dynamic voltage-current characteristic obtained by high-frequency sinusoidal modulation of the applied voltage is shown.

For comparison to the model the experiment was performed on the collector. Initial data: speed 1000 rpm, press force 20 N, voltage 4 V. Fig. 6 corresponds to the experimental oscillogram in Fig. 7.

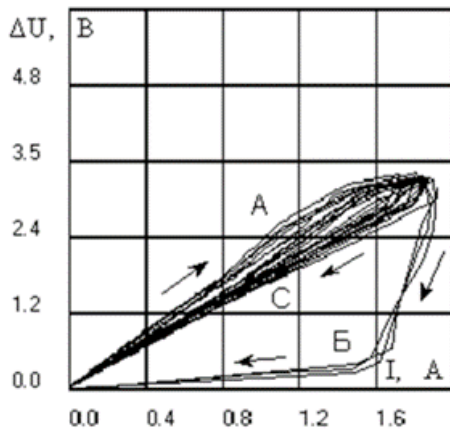


Fig. 6. Theoretical voltage-current attractor.

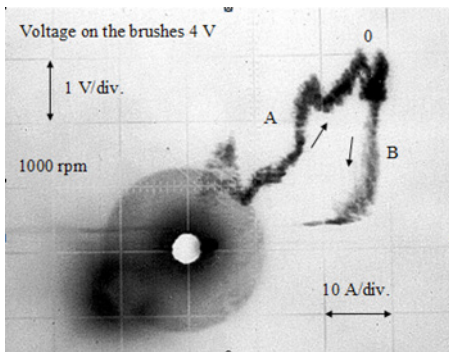


Fig. 7. The voltage-current attractor recorded during the passage of the collector lamella under the brush.

The simulation program allows to observe movement and development of the interacting microreliefs, aggregation of conducting clusters in the contact transition layer and the non-stationary temperature field. Fig. 8 shows examples of images obtained in the modelling process.

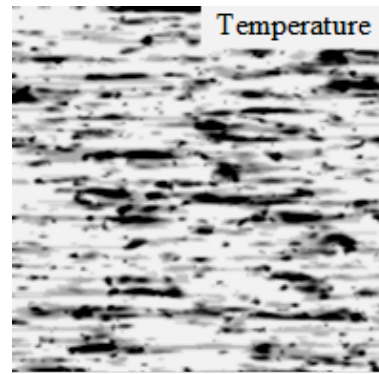
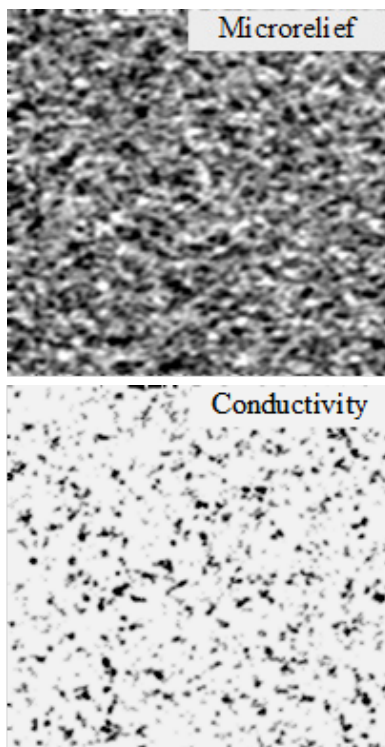


Fig. 8. Typical simulation images of the EFI synergistic model.

Fig. 9 shows enlarged fragments of the conduction in the contact transition layer, which contain characteristic conducting clusters. The shade portraits of the thermal field corresponding to the areas of conductivity show the values of local temperatures in various contact zones.

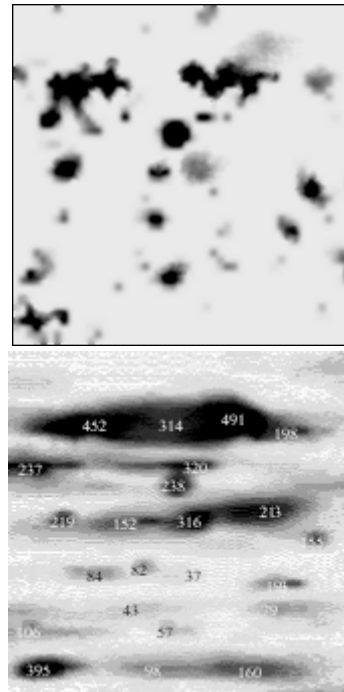


Fig. 9. Enlarged fragments of the conductivity containing characteristic contact clusters, and temperature field with indication of local temperatures (press force 30 N, voltage 2.5 V, velocity 30 m/s, contact is "brush EG-4 – steel").

Many conducting clusters have an oval or circular configuration. Usually they are located in less saturated areas with a relatively low average temperature. In the areas of increased heating a significant part of the clusters has a larger size and a complex configuration characterized by fractional fractal dimension. In addition, thermal zones are strongly elongated by the axis of the contact surface motion.

V. CONCLUSIONS

The structure of conductivity and thermal field is significantly influenced by the value of thermal conductivity of contact pair materials.

At low thermal conductivity the heated zones are elongated by the axis of contacting bodies movement and

take the form of diffuse strips.

With high thermal conductivity thermal zones acquire the local forms and at the same time have a lower temperature.

When certain values of the voltage and the press force are reached the temperature of a large number of thermal clusters reaches values at which the melting of the lower-melting material of the contact pair occurs. In practice, such modes of operation should be accompanied by increased sparking caused by the spitting of molten metal particles from the contact zone.

Most conductive clusters located in areas with low average temperature are oval or round in shape.

Clusters located in zones with a high average temperature have a larger size and a complex configuration characterized by fractional fractal dimension.

With an increase in the press force (F) the current, the saturation of the contact layer with conducting clusters, the number and temperature of the heated spots quickly increase.

Increasing the voltage at U increases the density of conductive clusters at a lesser degree, however it affects the temperature field almost the same way as press force.

REFERENCES

- [1] G. Haken, *Sinergetika*. M.: Mir, 1980.
- [2] I. M. Yaglom, *Sovremennaya kulytura I kompyutery*. M.: Nauka, 1990.
- [3] B. R. Fuller, *Sinergetics*. N.Y.: MacMillan, 1982.
- [4] G. Haken *Informatsiya i samoorganizatsiya. Makroskopicheskiy podhod k slozhnym sistemam*. M.: Mir, 1991.
- [5] S. V. Emelyanov, V. I. Utkin V. A. Taran i dr., *Teoriya sistem s peremennoy strukturoy*. M.: Nauka, 1970.
- [6] Г. П. Гладышев, *Термодинамика и макрокинетика природных иерархических процессов*. М.: Наука, 1988.
- [7] B. B. Mandelbrot, *The fractal geometry nature*. N.Y.: Freeman, 1983.
- [8] E. Feder, *Fraktaly*. M.: Mir, 1991.
- [9] B. M. Smirnov, *Fizika fraktalnykh klasterov*. M.: Nauka, 1991.
- [10] *Fraktaly v fizike, Trudy VI mezhdunarodnogo simpoziuma po fraktalam v fizike*. M.: Mir, 1988.
- [11] V. P. Isachenko, V. A. Osipova, A. S. Sukomel, *Teploperedacha*. M.: Energoizdat, 1981.
- [12] F. Kreit, U. Blek, *Osnovy teploperedachi*. M.: Mir, 1983.
- [13] I. M. Tetelybaum, Ya. I. Tetelynaum, *Modeli pryamoi analogii*. M.: Nauka, 1979.
- [14] I. M. Tetelybaum, Yu. R. Shneider, *Praktika analogovogo modelirovaniya dinamicheskikh sistem*. M.: Energoatomizdat, 1987.
- [15] V. A. Venikov, G. V. Venikov, *Teoriya podobiya i modelirovaniya (primenitelno k zadacham elektroenergetiki)*. M.: Vysshaya shkola, 1984.
- [16] A. Ilyin, I. Plokhov, I. Savraev, O. Kozyreva, N. Kotkov, "Forming and overlapping microreliefs in sliding contact simulation model," in *Environment. Technology. Resources: Proceedings of the 11th International Scientific and Practical Conference, Volume III, Rezekne: Latvia, 2017*, pp. 102–106, <http://dx.doi.org/10.17770/etr2017vol3.2532>
- [17] I. Plokhov, I. Savraev, A. Markov, A. Ilyin, O. Kozyreva, N. Kotkov, "Industrial tests of current distribution dynamics in the brush-contact apparatus of the turbo-generator," in *Environment. Technology. Resources, Rezekne, Latvia, Proceedings of the 11th International Scientific and Practical Conference, Volume III, Rezekne: Latvia, 2017*, pp. 258–268, <http://dx.doi.org/10.17770/etr2017vol3.2661>
- [18] O. Kozyreva, I. Plokhov, N. Kotkov, I. Savraev, A. Ilyin, "Experimental investigations of effect of LC-circuits on sparking and thermal state of sliding electric contact unit," in *Environment. Technology. Resources, Rezekne, Latvia, Proceedings of the 11th International Scientific and Practical Conference, Volume III, Rezekne: Latvia, 2017*. pp. 150–153, <http://dx.doi.org/10.17770/etr2017vol3.2575>
- [19] O. Kozyreva, I. Plokhov, I. Savraev, A. Ilyin, "Reducing sparking in the transient layer of the sliding electrical contact unit," in *2018 19th International Scientific Conference on Electric Power Engineering (EPE), 16–18 May 2018, Brno, Czech Republic, 2018*, pp. 189–193, <https://doi.org/10.1109/EPE.2018.8395969>
- [20] O. Kozyreva, Y. Guravlev, I. Plokhov, I. Savraev, A. Ilyin, "The regions of parametric instability of brush-contact device electromagnetic circuit in unstable working conditions," in *Environment. Technology. Resources. Proceedings of the 10th International Scientific and Practical Conference, Volume 1, Rezekne, Latvia, 2015*, pp. 84–88, <http://dx.doi.org/10.17770/etr2015vol1.218>
- [21] A. Ilyin, I. Plokhov, I. Savraev, O. Kozyreva, "Modeling of time dependent thermal process in sliding electrical microcontact," in *Environment. Technology. Resources. Proceedings of the 10th International Scientific and Practical Conference, Volume 3, Rezekne, Latvia, 2015*, pp. 109–113, <http://dx.doi.org/10.17770/etr2015vol3.194>
- [22] I. Plokhov, A. Ilyin, O. Kozyreva, I. Savraev, "The simulation model of sliding contact with three degrees of freedom and distributed parameters of the transition layer," in *Environment. Technology. Resources. Proceedings of the 10th International Scientific and Practical Conference, Volume 3, Rezekne, Latvia, 2015*, pp. 182–186, <http://dx.doi.org/10.17770/etr2015vol1.229>